

RESEARCH PAPER

OPEN ACCESS 

CircSEC24A (hsa_circ_0003528) interference suppresses epithelial-mesenchymal transition of hepatocellular carcinoma cells via miR-421/MMP3 axis

Bo Zhang^a and Jian Zhou^b

^aDepartment of Basic Medicine, Chongqing Medical and Pharmaceutical College, Chongqing, China; ^bDepartment of Pathology, The Affiliated Hospital of Southwest Medical University, Luzhou, Sichuan, China

ABSTRACT

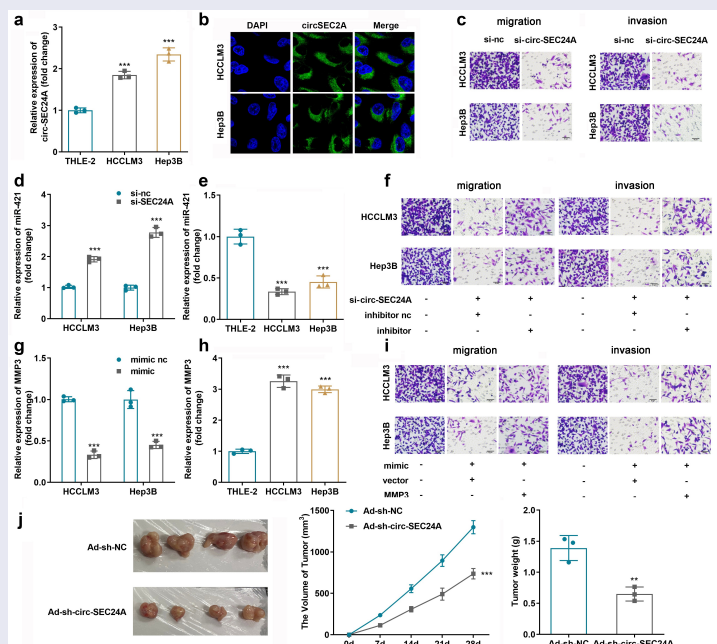
Accumulating evidence indicates that circular RNAs (circRNAs) function as conclusive modulators in diverse tumors, including in hepatocellular carcinoma (HCC). Nonetheless, knowledge of the latent mechanisms involving circRNAs in HCC development is insufficient. circSEC24A (hsa_circ_0003528) was discovered by microarray analysis of patients with HCC. Binding sites between circSEC24A, miR-421, miR-421 and matrix metalloproteinase 3 (MMP3) were predicted using online bioinformatics tools. Interactions involving miRNA and target genes or circRNAs were verified by luciferase reporter-gene and RNA pull-down assays. Two HCC cell lines (HCCLM3 and Hep3B) and normal THLE-2 liver cells were used for *in vitro* experiments. miRNA and mRNA expression levels were detected by RT-qPCR, and protein expression was measured by western blotting. Cell proliferation was evaluated using Cell Counting Kit 8 (CCK-8) assays along with colony formation assays. Cell invasion and migration were determined using the Transwell and wound healing migration assays. A xenograft model was used to evaluate the role of circSEC24A *in vivo*. circSEC24A expression was significantly upregulated in HCCLM3 and Hep3B cells. Silencing circSEC24A mitigated the proliferation, migration, invasion, and epithelial-mesenchymal transition (EMT) of HCC cells, which was abrogated by downregulation of miR-421. Meanwhile, MMP3 could bind to miR-421 to decrease the functional effects of miR-421 and induce tumor metastasis. Knockdown of circSEC24A suppressed tumor growth *in vivo*. circSEC24A interference suppressed HCC cell EMT by sponging miR-421, further regulating MMP3, and inhibiting tumor growth *in vivo*. Therefore, circSEC24A could represent a potential target for HCC patient treatment.

ARTICLE HISTORY

Received 18 January 2022
Revised 11 March 2022
Accepted 14 March 2022

KEYWORDS

hepatocellular carcinoma (HCC); circSEC24A; hsa_circ_0003528; miR-421; MMP3; competing endogenous RNA



Introduction

Hepatocellular carcinoma (HCC) is one of the most widely recognized cancers, with high incidence, mortality, and recurrence [1–3]. It has an insidious onset at an early stage, and there remains a lack of effective and reliable early screening [1–3]. Over the past three decades, despite significant advances in surgery and other treatment techniques, the five-year survival rate for HCC is still very poor, resulting in severe economic losses and a heavy social burden [4]. The initiation and progression of HCC involves multiple genes and environmental factors. Multiple pathological stages and changes involving various molecular events are required to realize the evolution of normal hepatocytes into HCC cells and even for eventual metastasis [5,6]. Therefore, it is vital to explore the underlying molecular mechanisms.

Previous studies have shown that epithelial-to-mesenchymal transition (EMT) is associated with cell polarity and cellular motor abilities. EMT is involved in the regulation of malignant biological behaviors of tumors [7,8]. The most significant molecular event during EMT is a decrease in E-cadherin expression and augmentation of N-cadherin and vimentin expression [9,10]. Recent studies have uncovered the fundamental function of EMT in HCC metastasis [11,12], highlighting the need to further investigate the molecular mechanisms involved in EMT in HCC.

Covalently closed circular RNAs (circRNAs) are non-coding RNAs connected by the back-splicing of exons (3' and 5' ends) or introns of precursor mRNAs, which are ubiquitously expressed in eukaryotes [13]. Recently, various studies have identified circRNAs as diagnostic and therapeutic targets for modulating tumor progression and metastasis [14,15]. In HCC, several circRNAs have been clarified to be involved in HCC progression, e.g. circ-SOX5 [16], circZFR [17]. Different from circRNAs's structure, miRNAs are another cluster of small non-coding RNAs which have a length of ~22 nucleotides [18], which considered to be important mediators in many biological process involved in HCC progression [19]. More importantly, alterations affecting circRNA expression have been reported to be linked to EMT to modulate tumor metastatic behavior

[20,21]. circSEC24A is a newfound circRNA that has been reported to accelerate tumor progress in squamous cell carcinoma [22] and pancreatic cancer [23]. However, the function of circSEC24A in HCC is indistinct.

In this study, the expression profile of circRNAs in patients with HCC was investigated, and circSEC24A (circBase ID: hsa_circ_0003528) was found to be abnormally expressed in HCC using bioinformatics tools. Our in-depth study demonstrated that circSEC24A features HCC metastasis through the miR-421–MMP3 axis *in vitro* and *in vivo*.

Materials and methods

Microarray analysis

The GSE94508 dataset obtained from the GEO database was employed to select for differential expression analysis in HCC patients. The online software tool GEO2R was applied to the filtrate of dysregulated circRNAs [24]. $|\text{fold change}| \geq 2$ and $p < 0.05$ were set as the criteria to identify significant differentially expressed circRNAs. Then, we identified the gene source of circRNA in circBase (<http://www.circbase.org/>) according to the sequence of the most significantly up-regulated circRNA to determine the name of the circRNA. Additionally, predicted binding sites between circRNA, miRNA, and target genes were performed by the online tool Starbase v.3.0 (<https://starbase.sysu.edu.cn/>) and TargetScan v.7.2 (http://www.targetscan.org/mmu_72/).

Patients

In total, 37 pairs of HCC and adjacent normal tissues were surgically removed from patients undergoing primary HCC surgery in the Affiliated Hospital of Southwest Medical University. Written informed consent was obtained from all patients, and the study was approved by the ethics committee and was conducted in accordance with the Declaration of Helsinki.

Cell lines

Two HCC cell lines (HCCLM3 and Hep3B) and normal THLE-2 hepatocytes were purchased from Shanghai Cell Bank, Chinese Academy of Sciences. HCC cell lines were maintained in DMEM

(Thermo Fisher Scientific, CA, USA), while normal hepatocytes were cultured in RPMI-1640 medium (Thermo Fisher Scientific) supplemented with 10% fetal bovine serum (FBS; Jiangsu Ningyan Biomedical Research Institute Co. Ltd, Jiangsu, China) in a 5% CO₂ incubator at 37°C.

Fluorescence in situ hybridization (Fish)

A total of 10⁴ HCC cells were planted in 96-well plates. After the cells adhered to the wall, 4% paraformaldehyde was added to fix the cells (15 min), followed by 0.1% Buffer A (15 min), Buffer C (30 min), 70% ethanol (3 min), 85% ethanol (3 min), and anhydrous ethanol (3 min). The probe was diluted with Buffer E, and incubated at 73°C for 5 min. After cooling, 100 µl of probe dilution was added to each well, and hybridized overnight at 37°C. Then Buffer F and Buffer C were successively added, DAPI working solution was added to avoid light staining for 20 minutes, and the location of circRNA in cells was determined under fluorescence microscope.

Oligonucleotide transfection

All small interfering RNAs (siRNAs), including si-circSEC24A#1, si-circSEC24A#2, corresponding negative control (si-NC), miR-421 mimic (mimic) and corresponding control (mimic NC), miR-421 inhibitor (inhibitor) and corresponding control (inhibitor NC), MMP3 overexpression vector (MMP3), and corresponding control (vector) were obtained from VectorBuilder Biotech (Jiangsu, China). Cell transfection was performed using Lipofectamine 3000 [25] (Invitrogen, Carlsbad, CA, USA) in accordance with the manufacturer's specifications until confluency reached 60%. After 24 h, the transfection efficiency was evaluated by quantitative reverse transcription polymerase chain reaction (RT-qPCR).

RT-qPCR assay

mRNA and miRNA expression levels were determined by RT-qPCR, and all PCRs were performed in triplicate. TRIzol reagent (Beyotime Biotech, Jiangsu, China) was used to extract RNA from HCCLM3, Hep3B, and THLE-2 cells. RNA integrity and concentration were assessed using a spectrophotometer (NanoDrop Technologies, Thermo Fisher Scientific) as reported [26]. The quantified RNA was then reverse-transcribed using the SuperScript IV CellsDirect cDNA kit (Thermo Fisher Scientific). Quantitative polymerase chain reaction was carried out on an ABI StepOnePlus Real-Time PCR System/Applied Biosystems 7500 Real-Time PCR system (Thermo Fisher Scientific). All primers were synthesized by Nanjing GenScript Biotech (Jiangsu, China) and were as follows in Table 1. The expression levels of circSEC24A and MMP3 were normalized to that of GAPDH, and U6 was used as an endogenous reference for miR-421 abundance.

Cell proliferation assays

Cell Counting Kit 8 (CCK-8; Beyotime Biotech) assays were used to measure cell viability from OD₄₅₀ absorbance readings (Spectra Max 250 spectrophotometer; Molecular Devices, California, USA). After exponential phase, cells were seeded into 96-well plates, 10 µl CCK-8 reagent was added to each well at 6, 24, 48, 72, and 96 h [27]. After 1.5 h of incubation, absorbance was measured using a microplate reader. Each experiment was performed independently in triplicate.

Colony formation assays were performed to determine the colony numbers. Briefly, HCC cells were seeded into 6-well plates and maintained for 14 days. Emergent cell colonies were then fixed and incubated with 0.1% crystal violet and 20% methanol solution for 10 min. Visible colonies were photographed and counted using a microscope

Table 1. Primer sequence.

Primer	Forward	Reverse
circSEC24A	5'-GCTCTCCTTAAACAGGATATACACAA-3'	5'-TGTCCTGAGAAGGAATAAGTCA-3'
miR-421	5'-GTCGCGCGGGUUAUUGCCTC-3'	5'-GGACATUAGUUGUCUGUAAATAG-3'
MMP3	5'-AGTCTTCCAATCCTACTGTTGCT-3'	5'-TCCCCTCACCTCCAATCC-3'
GAPDH	5'-AATGGACAACCTGGTCTGGAC-3'	5'-CCCTCCAGGGGATCTGTTTG-3'
U6	5'-AAAGCAAATCATCGGACGACC-3'	5'-GTACAACACATTGTTTCTCGGA-3'

(Nikon, Tokyo, Japan). All experiments were performed at least thrice.

Transwell assay

Cell migration and invasion abilities were measured using Transwell assays [28]. Cells (2×10^4 cells/well) and 200 μ l serum-free medium were added to the upper chamber of 24-well Transwell chambers (Corning, New York, USA). Medium (600 μ l) containing 2% FBS was added to the bottom chambers to chemically attract the upper cells. The cells were incubated for 24 h in migration assays, and 48 h in invasion assays with Matrigel (BD Bioscience, California, USA). After the cells migrated or invaded through the membranes, they were stained with 0.5% crystal violet. The number of migrated or invaded cells was counted under a $200 \times$ microscope in three random fields.

Wound healing migration assay

Wound healing migration assay was used to assess the migration ability of HCC cells, 6 orifice cells covered by more than 90%, pipetting spear with straightedge perpendicular scratches inside the cell culture plate, each hole through the five line, scratches with PBS rinse cells after three times, cleared cross out the adherent cells, add transfection of cells after serum free medium, watch pictures after 0 h, After incubation at 37°C in a 5% CO₂ incubator for 24 h, samples were taken again for observation and photographs were taken under an inverted fluorescence microscope.

Western blot assay

The protein levels in HCC cells were detected by western blot assays, and primary antibodies were used for this assay, including anti-N-cadherin (ab76011) and anti-E-cadherin (ab40772) (1/10,000, Abcam, USA). The cells were collected and lysed in RIPA buffer (Beyotime Biotech). The BCA Protein Assay kit (Beyotime Biotech) was used to measure protein concentrations [29]. Proteins were separated by 12% SDS-PAGE and transferred onto nitrocellulose membranes (Biosharp, Anhui, China) after electrophoretic

resolution. Subsequently, the membranes were sealed in 5% nonfat milk powder with TBS and 0.01% Tween and incubated with primary antibodies at 4°C overnight. Next, the membrane was incubated with secondary antibody for 1 h. Finally, an enhanced chemiluminescence kit (Beyotime Biotech) was used to visualize protein bands.

Luciferase reporter-gene assay

HCCLM3 and Hep3B cells were seeded in 24-well plates overnight until cell confluence reached approximately 60%. Wild-type and mutant circSEC24A luciferase reporter-gene constructs containing the binding site for miR-421 were cloned into pGL3-control vector (Promega, Madison, WI, USA). Then, 250 ng of luciferase reporter was transfected into HCCLM3 and Hep3B cells with miR-421 mimic using Lipofectamine 3000 (Invitrogen). After transfecting for 48 h, firefly and Renilla luciferase fluorescence were measured using the Dual-Luciferase Reporter Assay kit (Promega). The binding relationship involving MMP3 and miR-421 was studied in a similar way [30].

RNA pull-down assay

RNA pull-down assays were performed as previously described [31]. HCC cells were lysed and incubated with a biotinylated miR-421 probe and a negative control. Streptavidin-labeled magnetic beads (RNA Pull Down Assay Kit; 297-77,501; Whatman, UK) were added and cultured overnight at 4°C. RNA-protein complexes were eluted, resolved by SDS-PAGE, and stained with Silver Stain Plus (Beyotime Biotech). The results were determined by RT-qPCR.

Xenograft animal model assay

Twelve BALB/c nude mice (male, 4-weeks-old) were purchased from Shanghai SLAC Laboratory Animal Center (Shanghai, China). Animal experiments met the demands of laboratory animal welfare and ethics. Hep3B cells transfected with sh-NC or sh-circSEC24A suspended in DMEM at 2×10^6 were injected into the backs of mice and

allowed to grow for 25 days to establish the xenograft model. 7–10 days after inoculation, the maximum and minimum diameters of the tumor were measured with vernier calipers twice a week, and tumor volume was estimated (volume = maximum and minimum diameters $^2/2$).

Statistical analysis

All experiments were conducted thrice. GraphPad Prism 8.3 (GraphPad, CA, USA) and SPSS 19.0 (IBM, New York, USA) were used for data analysis. All data are shown as means \pm SD. Differences were analyzed using Student's *t*-test and one-way analysis of variance (ANOVA). Statistical significance was set at $p < 0.05$.

Results

Identification of aberrant expression of circSEC24A

We summarized differentially expressed circRNAs (DECs) obtained from the GSE94508 microarray dataset. As shown in the volcano map, 560 DECs were identified, including 214 up-regulated and 346 down-regulated circRNAs (Figure 1a). circRNA hsa_circ_0003528 (circSEC24A) was found to be the most significantly upregulated in HCC samples compared to that in controls (Figure 1b), which was verified in cell experiments. circSEC24A was markedly overexpressed in HCCLM3 and Hep3B cells (Figure 1c). Additionally, circSEC24A was found to be localized in the cytoplasm of HCC cells (Figure 1d).

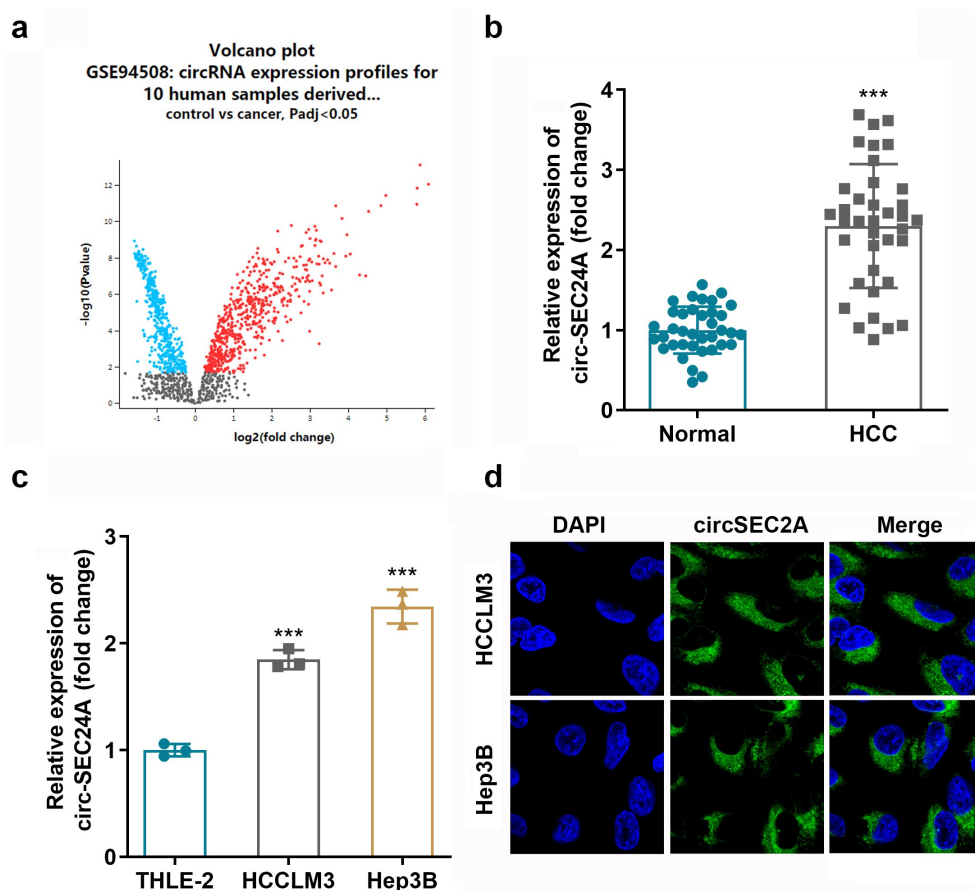


Figure 1. Aberrant expression level of circSEC24A in HCC. A Differentially expressed circRNAs in HCC clinical samples analyzed using an online dataset. B Expression of circSEC24A in HCC tissues and paracancer tissues measured by RT-qPCR. C Expression of circSEC24A in HCC cells measured by RT-qPCR. D The location of circSEC24A in HCC cells accessed by FISH method. *** $p < 0.001$.

Silencing circSEC24A inhibited HCC cell proliferation, invasion, migration and EMT

Then, whether circSEC24A can regulate aggressive behaviors were investigated after knocking down of circSEC24A. si-circSEC24A plasmids were transfected into HCCLM3 and Hep3B cells to suppress the expression of circSEC24A, demonstrating that circSEC24A was decreased more extensively after

transfection with si-circSEC24A 2# plasmid (Figure 2a). The proliferation, invasion, and migration of both HCCLM3 and Hep3B cells were assessed by CCK-8, colony formation, transwell, scratch test methods, and the results indicated that downregulation of circSEC24A significantly inhibited the proliferation, invasion, and migration of HCCLM3 and Hep3B cells compared to those in the control group (Figure 2b-e,

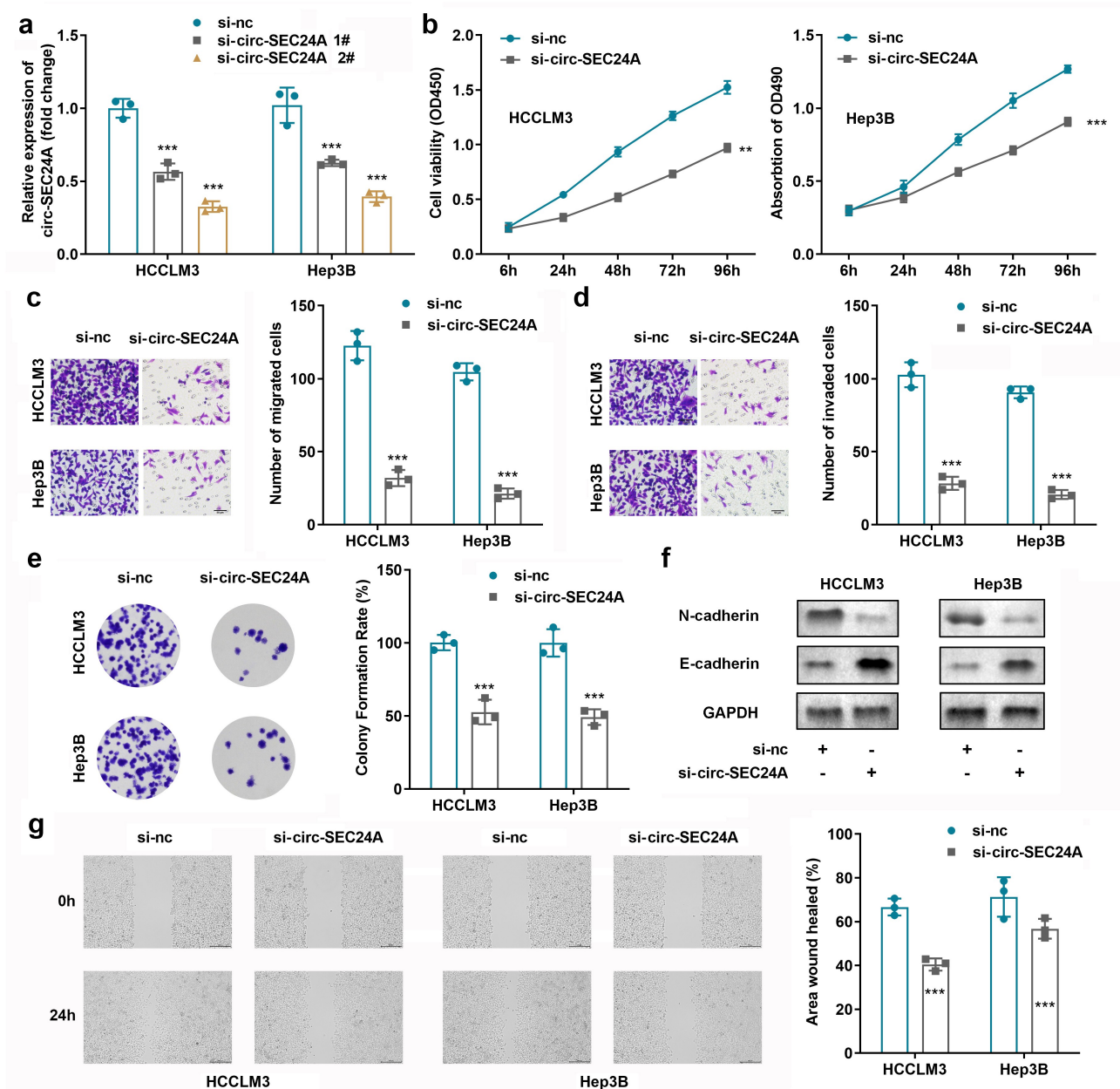


Figure 2. Suppressed circSEC24A cellular functions on HCC cells. A CircSEC24A expression was detected after transfection with interference plasmids. B Cell viability was detected using CCK8 assays. C-D. Cell migration and invasion abilities were assessed using Transwell assays. E. Colony formation assays were applied to detect cell proliferation. F. Expression of EMT-related proteins was detected by western blot. G. Wound healing migration assay was performed to measure cell migration ***p < 0.01, ****p < 0.001, vs. si-NC group.

g). Meanwhile, western blot analysis demonstrated that N-cadherin protein was downregulated, while E-cadherin protein was upregulated by silencing circSEC24A (figure 2f).

CircSEC24A functioned as a sponge for miR-421

miR-421 was predicted to be a target of circSEC24A using the online tool Starbase v.3.0; the binding sites are illustrated in Figure 3a. Luciferase activity of both HCCLM3 and Hep3B cells was dramatically

suppressed in cells transfected with the miR-421 mimic and wild-type circSEC24A (Figure 3(b,c)). RNA pull-down assays demonstrated that circSEC24A could be pulled-down by biotinylated miR-421 (Figure 3(d,e)). Moreover, the expression level of miR-421 appeared to be suppressed in HCC tissues (figure 3f) and two HCC cell lines (Figure 3g) tested relative to normal groups. Additionally, the expression level of miR-421 was significantly upregulated when circSEC24A expression was suppressed (Figure 3h).

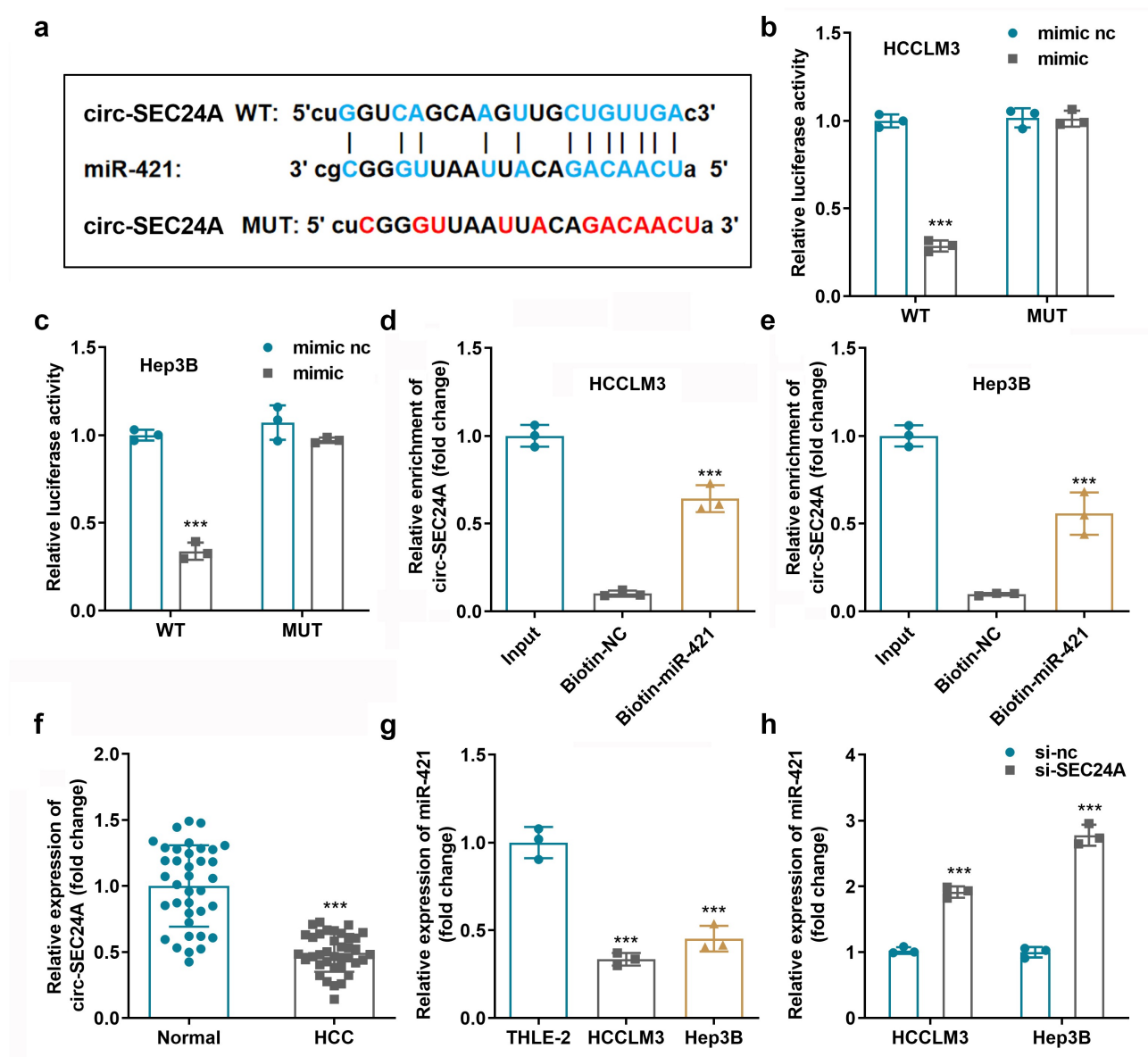


Figure 3. miR-421 bound circSEC24A. A Binding sites involving miR-421 and circSEC24A predicted by bioinformatic analysis. B-C. Luciferase reporter assays were conducted to confirm interactions between miR-421 and circSEC24A. D-E. Interaction between miR-421 and circSEC24A was verified using RNA pull-down assays. F. miR-421 expression in HCC tissues and paracancer tissues measured by RT-qPCR. G. miR-421 expression in HCC cells measured by RT-qPCR. H. miR-421 expression was measured after circSEC24A knockdown. *** $p < 0.001$, vs. mimic NC, si-NC, Biotin-NC, THLE-2 and normal group.

CircSEC24A may accelerate aggressiveness of HCC progression by regulating miR-421

Next, we assessed aggressiveness of HCC cells by inhibiting miR-421. As indicated in Figure 4a, miR-421 expression was sharply suppressed in the miR-421 inhibitor group and increased in the miR-421 mimic cohort in both HCCLM3 and Hep3B cells. Downregulation of miR-421 partially abrogated the effects of circSEC24A on the proliferation, migration, invasion, and EMT of HCC cells (Figure 4b-g).

MMP3 as a target of miR-421

MMP3 is a target gene of miR-421 according to the online tool TargetScan v.7.2, and its binding sites are illustrated in Figure 5a. The results of luciferase and RNA pull-down assays confirmed the binding relationship involving MMP3 and miR-421 (Figure 5b-e). The expression of MMP3 mRNA was notably increased in HCC tissues and cells compared to that in normal groups (Figure 5(f,g)). Moreover, mRNA expression of MMP3 was prominently reduced by the miR-421 mimic (Figure 5h).

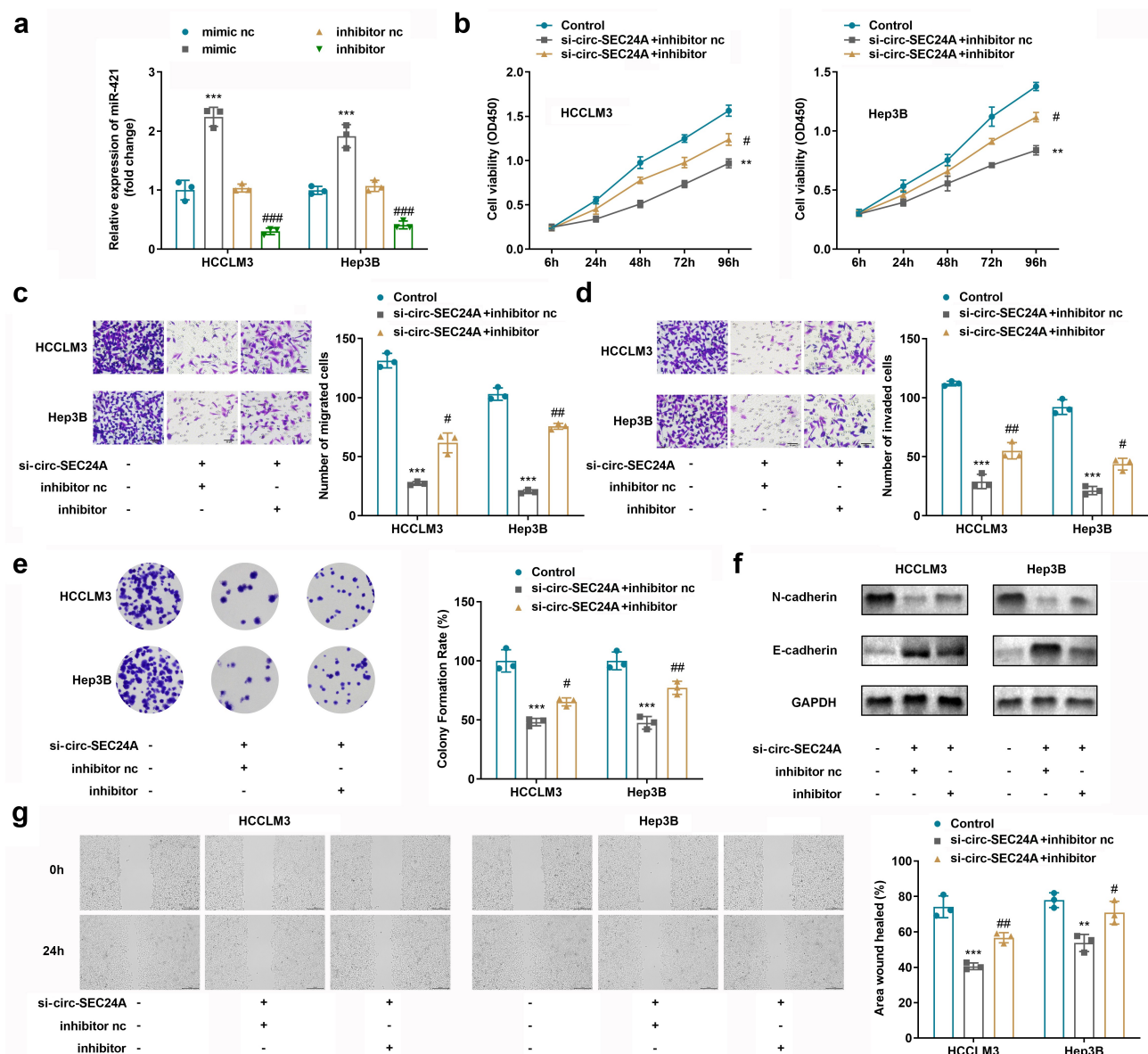


Figure 4. Effects of miR-421 inhibitor on HCC cells. A. miR-421 expression levels were detected by RT-qPCR. B Cell viability was determined using CCK8 assays. C-D. Cell migration and invasion abilities were assessed using Transwell assays. E. Colony formation assays were applied to detect cell proliferation. F. Expression of EMT-related proteins were detected by western blotting. G. Wound healing migration assay was performed to measure cell migration. ** $p < 0.01$, *** $p < 0.001$, vs. mimic NC, control group. # $p < 0.05$, ## $p < 0.01$, ### $p < 0.001$, vs. inhibitor NC, si-circSEC24A + inhibitor group.

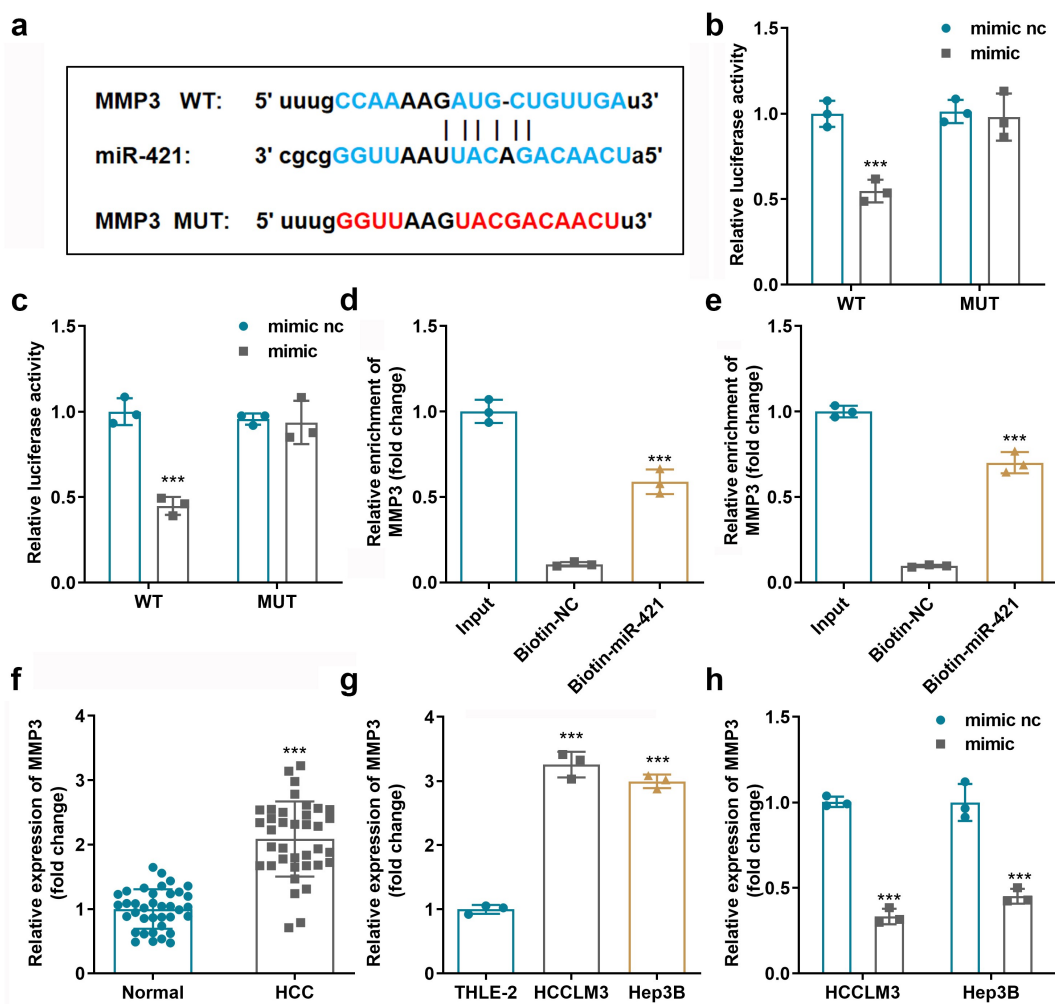


Figure 5. MMP3 as a miR-421 target gene. **A** Bioinformatic analysis predicted binding sites involving miR-421 and MMP3. **B-C.** Luciferase reporter-gene assays were conducted to confirm interactions between miR-421 and MMP3. **D-E.** Interaction between miR-421 and MMP3 was verified using RNA pull-down assays. **F.** MMP3 expression in HCC tissues and paracancer tissues measured by RT-qPCR. **G.** MMP3 expression in HCC cells measured by RT-qPCR. **H.** MMP3 expression was measured after miR-421 up-regulation. *** $p < 0.001$, vs. mimic NC, si-NC, Biotin-NC, THLE-2 group.

Over-expressed MMP3 inhibited the effects of miR-421

To investigate the effects of MMP3 on miR-421, we overexpressed MMP3 by transfecting OE-MMP3 plasmid into HCCLM3 and Hep3B cells. As revealed in Figure 6a, co-transfection with miR-421 overexpression plasmid and the OE-MMP3 vector accelerated cell proliferation (Figure 6 b and e), migration (Figure 6 c,g), invasion (Figure 6d), and the EMT process (figure 6f) in HCC cells. Furthermore, upregulated MMP3 partly antagonized the cellular functions of miR-421 in HCC cells.

Depletion of circSEC24A inhibited tumor growth in vivo

To elucidate the function of circSEC24A in HCC, a xenograft tumor model was established, and tumor volumes and weights were analyzed. As revealed in Figure 7d, two sh-circSEC24A plasmids obviously suppressed circSEC24A expression *in vivo*, which was more potent in 1# group (Figure 7d). What's more, miR-421 could also be elevated while MMP was suppressed *in vivo* by inhibition of circSEC24A (Figure 7(e,f)). Additionally, the results showed that tumor volume (Figure 7a-b) and weight (Figure 7c) in

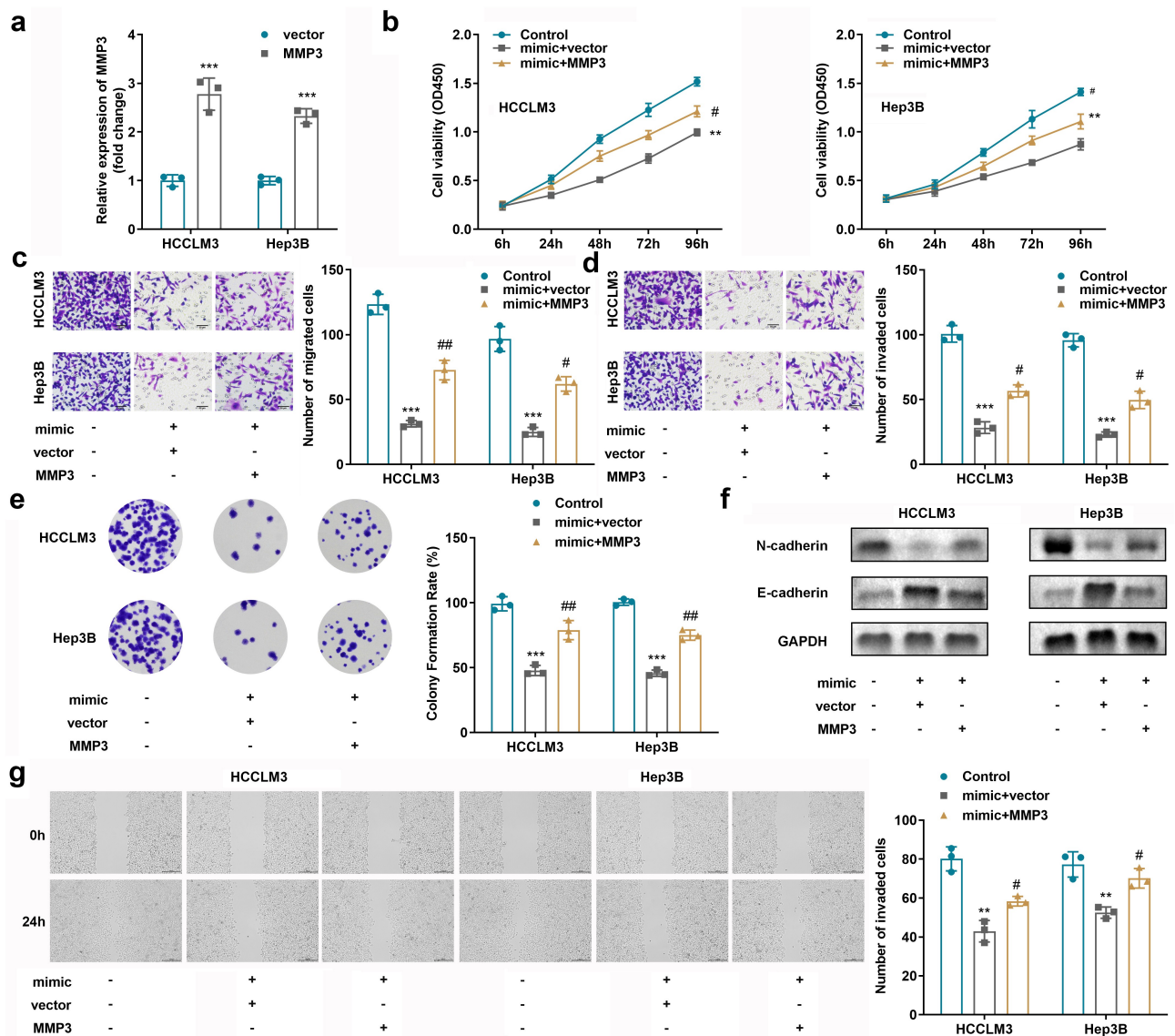


Figure 6. Elevated MMP3 levels mitigated the effects of miR-421. A. MMP3 expression was detected by RT-qPCR. B. Cell viability was detected using CCK8 assays. C-D. Cell migration and invasion were evaluated using Transwell assays. E. Colony formation assays were applied to detect cell proliferation. F. Expression of EMT-related proteins was detected by western blotting. G. Wound healing migration assay was performed to measure cell migration. ** $p < 0.01$, *** $p < 0.001$, vs. vector, control group. # $p < 0.05$, ## $p < 0.01$, vs. mimic+vector group.

the sh-circSEC24A group were significantly lower than those in the control group. Furthermore, protein levels of MMP3 and N-cadherin in tumor tissues were suppressed while E-cadherin was upregulated (Figure 7g).

Discussion

In this study, circSEC24A was abnormally elevated in HCC, and knockdown of circSEC24A inhibited cell proliferation, invasion, migration, and EMT

progression in *in vitro* functional assays. Our findings revealed that circSEC24A competes with MMP3 for miR-421 binding, thereby manipulating cell fate and promoting tumorigenesis.

Dysregulation of circRNAs, identified using RNA sequencing technologies along with online bioinformatic analysis has been reported to regulate the initiation and development of diverse disorders including HCC [15,32,33]. Numerous studies have suggested that certain circRNAs

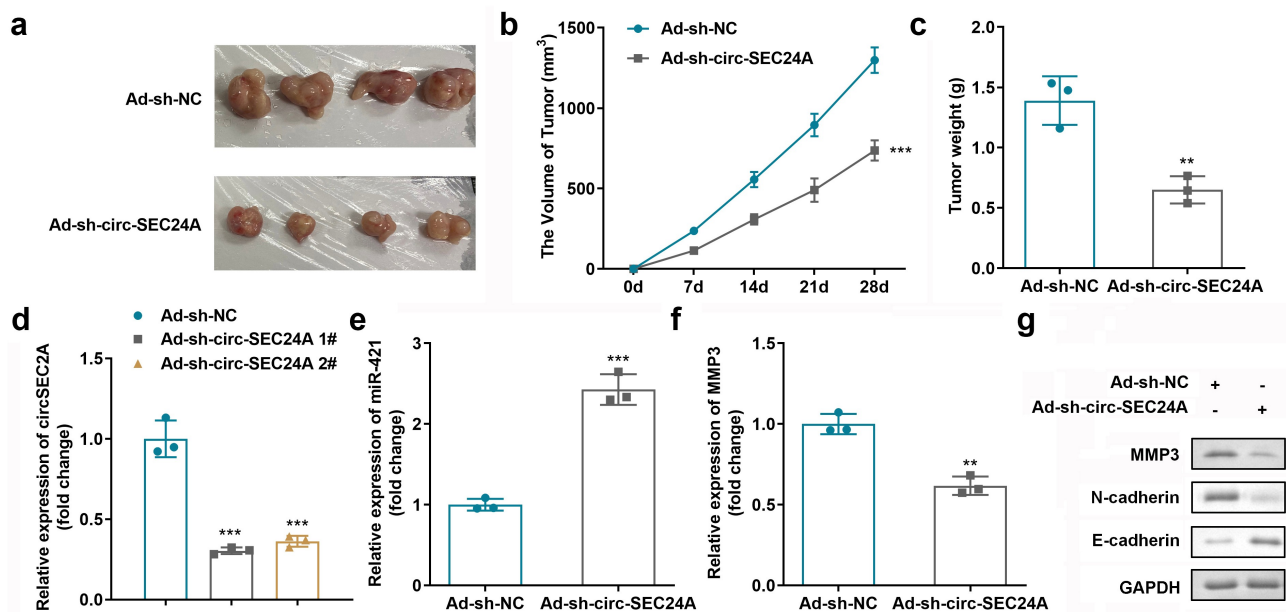


Figure 7. Effects of sh-circSEC24A on xenograft model *in vivo*. Representative images (a), tumor volumes (b), and tumor weights (c) of tumors derived from xenograft animal models. RT-qPCR analyses of (d) circSEC24A, (e) miR-421, and (f) MMP3 expression. (g) EMT related proteins were measured by western blotting assay. ** $p < 0.01$, *** $p < 0.001$, vs. Ad-sh-NC group.

influence the occurrence and development of HCC. For instance, over-expression of circRNA Cdr1as facilitates aggressive behavior of HCC cells by modulating miR-1270 [33]. Yao et al. [34] demonstrated that circ_0001955 expedites HCC carcinogenesis through competing endogenous RNA (ceRNA) mechanisms. Our study identified the potential role of circSEC24A in HCC. Functional assays indicated that silencing circSEC24A retarded HCC development by inhibiting the proliferation, migration, invasion, and EMT of HCC cells. *In vivo* experiments further showed that knockdown of circSEC24A suppressed tumor growth. Hence, circSEC24A has been postulated to act as an oncogene in HCC.

Emerging evidence has shown that circRNAs can act as ceRNAs and isolate specific miRNAs from target genes, thereby inhibiting miRNA stability and function [32,35]. Our data indicated that circSEC24A might bind to miR-421, which is known to play a crucial role in tumors. For instance, miR-421 serves as an oncogene in osteosarcoma [36], ovarian cancer [37], glioma [38], pancreatic cancer [39], ovarian cancer [40], and HCC [41], whereas a small fraction of the data show that miR-421 plays an oncogenic role in HCC [42]. Therefore, it is essential to identify the regulatory mechanism involving miR-421 in HCC.

Our study demonstrated that miR-421 levels were decreased in HCC cells, which is in accord with previous research results [41]. Moreover, inhibition of miR-421 abrogated the suppressive functional effects of silencing circSEC24A in HCC, indicating that circSEC24A downregulation inhibited the aggressiveness of HCC cells by upregulating miR-421.

Our data suggested that MMP3 binds to miR-421. MMP3 is a member of the MMP family, and alterations to MMPs *in vivo* play crucial roles in promoting tumor invasion and metastasis [43,44]. MMP3 has been reported to promote tumor invasion and metastasis in a variety of tumors [45–47], including HCC [48]. Wang et al. [48] showed that miR-30a-3p suppresses tumor formation by reducing the expression of MMP3 in HCC cells. Likewise, downregulation of miR-17 dramatically suppresses cell migration and invasion *in vitro* and *in vivo* by inhibiting MMP3 [49]. These studies demonstrate that MMP3 may play a positive role in tumor cell invasion and migration. In this study, MMP3 levels were elevated in HCC cells, and overexpression of MMP3 abrogated the effect of miR-421 on cell proliferation, invasion, and migration inhibition. Furthermore, EMT progression by cells was suppressed by upregulated MMP3, which is in accord with previous studies

[50,51]. Scheau et al. [52] reported that MMP3 participates in the EMT process in HCC and plays a role in promoting tumor invasion and metastasis, which is consistent with the findings of this study.

Conclusion

Collectively, these results suggest that circSEC24A interference suppresses HCC development by regulating the miR-421/MMP3 axis. Therefore, circSEC24A could represent a potential target for HCC patient treatment.

Ethical approval

This study protocol was approved by the Ethics Committee of the Affiliated Hospital of Southwest Medical University 201,900,128 on January 28th in 2019.

Disclosure statement

No potential conflict of interest was reported by the author(s).

Funding

The author(s) reported there is no funding associated with the work featured in this article.

References

- [1] European Association For The Study Of The Liver; European Organisation For Research And Treatment Of Cancer. EASL-EORTC clinical practice guidelines: management of hepatocellular carcinoma. *J Hepatol.* 2012 Apr 01;56(4):908–943.
- [2] Degasperis E, Colombo M. Distinctive features of hepatocellular carcinoma in non-alcoholic fatty liver disease. *Lancet Gastroenterol Hepatol.* 2016 Oct 01;1(2):156–164.
- [3] Liang Q, Shen X, Precision Medicine: SG. Update on diagnosis and therapeutic strategies of hepatocellular carcinoma. *CURR MED CHEM.* 2018 Jan 20;25(17):1999–2008.
- [4] Forner A, Reig M, Bruix J. Hepatocellular carcinoma. *LANCET.* 2018 Mar 31;391(10127):1301–1314.
- [5] Jiang H, Cao HJ, Ma N, et al. Chromatin remodeling factor ARID2 suppresses hepatocellular carcinoma metastasis via DNMT1-Snail axis. *Proc Natl Acad Sci U S A.* 2020 Mar 03;117(9):4770–4780.

- [6] Yang LY, Luo Q, Lu L, et al. Increased neutrophil extracellular traps promote metastasis potential of hepatocellular carcinoma via provoking tumorous inflammatory response. *J HEMATOL ONCOL.* 2020 Jan 06;13(1):3.
- [7] Pastushenko I, Blanpain C. EMT transition states during tumor progression and metastasis. *TRENDS CELL BIOL.* 2019 Mar 01;29(3):212–226.
- [8] Suarez-Carmona M, Lesage J, Cataldo D, et al. EMT and inflammation: inseparable actors of cancer progression. *MOL ONCOL.* 2017 Jul 01;11(7):805–823.
- [9] Paolillo M, Schinelli S. Extracellular matrix alterations in metastatic processes. *INT J MOL SCI.* 2019 Oct 07;20(19):4947.
- [10] Serrano-Gomez SJ, Maziveyi M, Alahari SK. Regulation of epithelial-mesenchymal transition through epigenetic and post-translational modifications. *MOL CANCER.* 2016 Feb 24;15:18.
- [11] Giannelli G, Koudelkova P, Dituri F, et al. Role of epithelial to mesenchymal transition in hepatocellular carcinoma. *J HEPATOL.* 2016 Oct 01;65(4):798–808.
- [12] Dong Y, Zheng Q, Wang Z, et al. Higher matrix stiffness as an independent initiator triggers epithelial-mesenchymal transition and facilitates HCC metastasis. *J HEMATOL ONCOL.* 2019 Nov 08;12(1):112.
- [13] Patop IL, Wust S, Kadener S. Past, present, and future of circRNAs. *EMBO J.* 2019 Aug 15;38(16):e100836.
- [14] Yu T, Wang Y, Fan Y, et al. CircRNAs in cancer metabolism: a review. *J HEMATOL ONCOL.* 2019 Sep 04;12(1):90.
- [15] Liu Z, Yu Y, Huang Z, et al. CircRNA-5692 inhibits the progression of hepatocellular carcinoma by sponging miR-328-5p to enhance DAB2IP expression. *CELL DEATH DIS.* 2019 Nov 27;10(12):900.
- [16] Cai Y, Circular JY. RNA SOX5 promotes the proliferation and inhibits the apoptosis of the hepatocellular carcinoma cells by targeting miR-502-5p/synoviolin 1 axis. *BIOENGINEERED.* 2022 Jan 01;13(2):3362–3370.
- [17] Zhou Y, Tang W, Zhuo H, et al. Cancer-associated fibroblast exosomes promote chemoresistance to cisplatin in hepatocellular carcinoma through circZFR targeting signal transducers and activators of transcription (STAT3)/ nuclear factor -kappa B (NF-kappaB) pathway. *BIOENGINEERED.* 2022 Mar 01;13(3):4786–4797.
- [18] Zhang X, Wang S, Wang H, et al. Circular RNA circNRIP1 acts as a microRNA-149-5p sponge to promote gastric cancer progression via the AKT1/mTOR pathway. *MOL CANCER.* 2019 Jan 01;18(1):20.
- [19] Nagy A, Lanczky A, Menyhart O, et al. Validation of miRNA prognostic power in hepatocellular carcinoma using expression data of independent datasets. *Sci Rep.* 2018 Jun 15;8(1):9227.

- [20] Conn SJ, Pillman KA, Toubia J, et al. The RNA binding protein quaking regulates formation of circ. RNAs. *CELL*. 2015 Mar 12;160(6):1125–1134.
- [21] Shang BQ, Li ML, Quan HY, et al. Functional roles of circular RNAs during epithelial-to-mesenchymal transition. *MOL CANCER*. 2019 Sep 16;18(1):138.
- [22] Lu X, Gan Q, Circular GC. RNA circSEC24A promotes cutaneous squamous cell carcinoma progression by regulating miR-1193/MAP3K9 axis. *Onco Targets Ther*. 2021 Jan 20;14:653–666.
- [23] Chen Y, Xu S, Liu X, et al. CircSEC24 upregulates TGFBR2 expression to accelerate pancreatic cancer proliferation and migration via sponging to miR-606. *CANCER CELL INT*. 2021 Dec 14;21(1):671.
- [24] Barrett T, Wilhite SE, Ledoux P, et al. NCBI GEO: archive for functional genomics data sets--update. *NUCLEIC ACIDS RES*. 2013 Jan 01;41:D991–5.
- [25] Lv R, Pan X, Song L, et al. MicroRNA-200a-3p accelerates the progression of osteoporosis by targeting glutaminase to inhibit osteogenic differentiation of bone marrow mesenchymal stem cells. *BIOMED PHARMACOTHER*. 2019 Aug 01;116:108960.
- [26] Hatzis C, Sun H, Yao H, et al. Effects of tissue handling on RNA integrity and microarray measurements from resected breast cancers. *J Natl Cancer Inst*. 2011 Dec 21;103(24):1871–1883.
- [27] Zhang Y, Zhang Y, Wang S, et al. SP1-induced lncRNA ZFPM2 antisense RNA 1 (ZFPM2-AS1) aggravates glioma progression via the miR-515-5p/Superoxide dismutase 2 (SOD2) axis. *BIOENGINEERED*. 2021 Jan 01;12(1):2299–2310.
- [28] Omar Zaki SS, Kanesan L, Leong MYD, et al. The influence of serum-supplemented culture media in a transwell migration assay. *CELL BIOL INT*. 2019 Jan 01;43(10):1201–1204.
- [29] Yin N, Zhu L, Ding L, et al. MiR-135-5p promotes osteoblast differentiation by targeting HIF1AN in MC3T3-E1 cells. *CELL MOL BIOL LETT*. 2019 Jan 20;24:51.
- [30] Cheng B, Rong A, Zhou Q, et al. LINC00662 promotes colon cancer tumor growth and metastasis by competitively binding with miR-340-5p to regulate CLDN8/IL22 co-expression and activating ERK signaling pathway. *J Exp Clin Cancer Res*. 2020 Jan 03;39(1):5.
- [31] Rinn JL, Kertesz M, Wang JK, et al. Functional demarcation of active and silent chromatin domains in human HOX loci by noncoding RNAs. *CELL*. 2007 Jun 29;129(7):1311–1323.
- [32] Han TS, Hur K, Cho HS, et al. Epigenetic Associations between lncRNA/circRNA and miRNA in hepatocellular carcinoma. *Cancers (Basel)*. 2020 Sep 14;12(9):2622.
- [33] Su Y, Lv X, Yin W, et al. CircRNA Cdr1as functions as a competitive endogenous RNA to promote hepatocellular carcinoma progression. *Aging (Albany NY)*. 2019 Oct 01;11(19):8183–8203.
- [34] Yao Z, Xu R, Yuan L, et al. Circ_0001955 facilitates hepatocellular carcinoma (HCC) tumorigenesis by sponging miR-516a-5p to release TRAF6 and MAPK11. *CELL DEATH DIS*. 2019 Dec 10;10(12):945.
- [35] Li X, Ding J, Wang X, et al. NUDT21 regulates circRNA cyclization and ceRNA crosstalk in hepatocellular carcinoma. *ONCOGENE*. 2020 Jan 01;39(4):891–904.
- [36] Liang X, Zhang L, Ji Q, et al. miR-421 promotes apoptosis and suppresses metastasis of osteosarcoma cells via targeting LTBP2. *J CELL BIOCHEM*. 2019 Mar 28;120:10978–10987.
- [37] Ye W, Ni Z, Yicheng S, et al. Anisomycin inhibits angiogenesis in ovarian cancer by attenuating the molecular sponge effect of the lncRNAMeg3/miR421/PDGFR α axis. *INT J ONCOL*. 2019 Dec 01;55(6):1296–1312.
- [38] Liu L, Cui S, Zhang R, et al. MiR-421 inhibits the malignant phenotype in glioma by directly targeting MEF2D. *AM J CANCER RES*. 2017 Jan 20;7(4):857–868.
- [39] Shopit A, Li X, Tang Z, et al. miR-421 up-regulation by the oleanolic acid derivative K73-03 regulates epigenetically SPINK1 transcription in pancreatic cancer cells leading to metabolic changes and enhanced apoptosis. *PHARMACOL RES*. 2020 Nov 01;161:105130.
- [40] Ren F, Shrestha C, Shi H, et al. Targeting of KDM5A by miR-421 in human ovarian cancer suppresses the progression of ovarian cancer cells. *Onco Targets Ther*. 2020 Jan 20;13:9419–9428.
- [41] Wang W, Li Y, Li X, et al. Circular RNA circ-FOXP1 induced by SOX9 promotes hepatocellular carcinoma progression via sponging miR-875-3p and miR-421. *BIOMED PHARMACOTHER*. 2020 Jan 01;121:109517.
- [42] Xu L, Feng X, Hao X, et al. CircSETD3 (hsa_circ_0000567) acts as a sponge for microRNA-421 inhibiting hepatocellular carcinoma growth. *J Exp Clin Cancer Res*. 2019 Feb 22;38(1):98.
- [43] Kessenbrock K, Plaks V, Werb Z. Matrix metalloproteinases: regulators of the tumor microenvironment. *CELL*. 2010 Apr 02;141(1):52–67.
- [44] Winer A, Adams S, Mignatti P. Matrix metalloproteinase inhibitors in cancer therapy: turning past failures into future successes. *MOL CANCER THER*. 2018 Jun 01;17(6):1147–1155.
- [45] Jin Y, Li Y, Wang X, et al. Dysregulation of MiR-519d affects oral squamous cell carcinoma invasion and metastasis by targeting MMP3. *J CANCER*. 2019 Jan 20;10(12):2720–2734.
- [46] Chen CL, Zhang L, Jiao YR, et al. miR-134 inhibits osteosarcoma cell invasion and metastasis through targeting MMP1 and MMP3 in vitro and in vivo. *FEBS LETT*. 2019 May 01;593(10):1089–1101.
- [47] Pittayapruek P, Meehansan J, Prapapan O, et al. Role of matrix metalloproteinases in photoaging and Photocarcinogenesis. *INT J MOL SCI*. 2016 Jun 02;17(6):868.

- [48] Wang W, Lin H, Zhou L, et al. MicroRNA-30a-3p inhibits tumor proliferation, invasiveness and metastasis and is downregulated in hepatocellular carcinoma. *Eur J Surg Oncol*. 2014 Nov 01;40(11):1586–1594.
- [49] Lin YH, Liao CJ, Huang YH, et al. Thyroid hormone receptor represses miR-17 expression to enhance tumor metastasis in human hepatoma cells. *ONCOGENE*. 2013 Sep 19;32(38):4509–4518.
- [50] Przybylo JA, Radisky DC. Matrix metalloproteinase-induced epithelial-mesenchymal transition: tumor progression at Snail's pace. *Int J Biochem Cell Biol*. 2007 Jan 20;39(6):1082–1088.
- [51] Zhang M, Dai C, Zhu H, et al. Cyclophilin A promotes human hepatocellular carcinoma cell metastasis via regulation of MMP3 and MMP9. *MOL CELL BIOCHEM*. 2011 Nov 01;357(1–2):387–395.
- [52] Scheau C, Badarau IA, Costache R, et al. The role of matrix metalloproteinases in the epithelial-mesenchymal transition of hepatocellular carcinoma. *Anal Cell Pathol (Amst)*. 2019 Jan 20;2019:9423907.